Analytical Investigations on the Mesh Stiffness Function of Solid Narrow Faced Spur and Helical Gears

Xiaoyu Gu, Philippe Velex, Philippe Sainsot, Jérôme Bruyère

ANALYTICAL INVESTIGATIONS ON THE MESH STIFFNESS FUNCTION OF SOLID NARROW FACED SPUR AND HELICAL GEARS

Xiaoyu Gu
Université de Lyon, LaMCoS, UMR CNRS 5259,
INSA de Lyon, Villeurbanne, France

Philippe Velex*
Université de Lyon, LaMCoS, UMR CNRS 5259,
INSA de Lyon, Villeurbanne, France
philippe.velex@insa-lyon.fr

Philippe Sainsot
Université de Lyon, LaMCoS, UMR CNRS 5259,
INSA de Lyon, Villeurbanne, France

Jérôme Bruyère
Université de Lyon, LaMCoS, UMR CNRS 5259,
INSA de Lyon, Villeurbanne, France

ABSTRACT

Approximate formulae are presented which give the time-varying mesh stiffness function for ideal solid narrow-faced spur and helical gears. The corresponding results compare very well with those obtained by using 2D finite element models and specific benchmark software codes thus validating the proposed analytical approach. More deviations are reported on average mesh stiffness which, to a large extent, are due to the modelling of gear body deflections.

NOMENCLATURE

b, contact width

k_0, average mesh stiffness per unit contact length

$k_M(\tau)$, mesh stiffness per unit contact length

$k_{m0} = k_0 \dfrac{b\varepsilon_\alpha}{\cos\beta_b}$, average mesh stiffness

$\hat{k}(\tau) = \dfrac{k(\tau)}{k_{m0}}$, dimensionless mesh stiffness function

$L(\tau)$, time-varying contact length

$Sinc(x) = \dfrac{\sin(\pi x)}{\pi x}$, sine cardinal function

α, relative variation in mesh stiffness amplitude

β_b, base helix angle

$\varepsilon_\alpha, \varepsilon_\beta$, profile and face contact ratios

$\varphi_M(\tau)$, functions representing the time variations of the mesh stiffness per unit contact length

$\tau = t/T_m$, normalized time with respect to the mesh period T_m

INTRODUCTION

Mesh stiffness and its time-variations are recognized as key parameters controlling gear dynamics and tooth loading to a large extent. A large number of results can be found in the literature which include the 2D models of Weber and Banaschek [1], Attia [2], Cornell [3], Winter and Poldleski [4], Sainsot et al. [5], Wilcox and Coleman [6], Chabert et al. [7] etc., the plate models of Umezawa [8], Yau et al. [9], Cai [10], the elastic foundation models of Seager [11], Schmidt et al. [12], Ajmi and Velex [13] and the more sophisticated 3D finite element models of Vedmar [14], Steward [15], Haddad [16], to name a few. One major difficulty is the necessity to simultaneously account for local and global scale phenomena such as contact and tooth structural deflections and define the relevant elastic domain of interest with the appropriate boundary conditions. From a more fundamental viewpoint, it should also be emphasized that the notion of mesh stiffness itself (defined as a single scalar function) is unclear when it comes to 3D situations.

*Address all correspondence to this author.

In this paper, the classic pseudo-3D thin-slice approach [17] is employed with the main objective of establishing some approximate analytical formulae representative of the mesh stiffness time variations for solid spur and helical gears. A number of comparisons with numerical simulations are presented which show that the proposed theory can give realistic results which can be useful at the early design stage and in the development of dynamic models.

I THEORY

In what follows, it is assumed that actual gears can be viewed as the superposition of infinitesimal (thin) gears in the face width direction which are staggered in the case of helical gears. The contacts between the pinion and the gear are line contacts which are sliced accordingly, thus leading to infinitesimal contact segments of length dM moving in translation in the base plane during the course of the meshing. A normal stiffness per unit contact length $k_M(\tau)$, possibly time (or position)-varying, is associated with every segment so that the overall mesh stiffness is given by the integral:

$$k(\tau) = \int_{L(\tau)} k_M(\tau)\, dM \qquad (1)$$

where $\tau = t/T_m$ is a normalized time with respect to the mesh period T_m and $L(\tau)$ is the time-varying contact length.

Each $k_M(\tau)$ function accounts for 3 stiffness elements in series which comprise the pinion and gear tooth structural stiffness (bending, fillet deflection, etc.) along with the contact stiffness. The formulation in (1) implicitly implies that all the stiffness elements $k_M(\tau)$ are in parallel along the contact lines hence that the inter-tooth elastic couplings are neglected. Another obvious limitation of this formulation is that the elastic couplings between the points of contact on the same tooth pair are ignored. This issue has been addressed by Seager [11], Ajmi and Velex [13], Steward [15] who have shown that such couplings can become influential on tooth load distribution but mostly in the vicinity of the tooth flank edges and corners. However, it has also been demonstrated that the dynamic response of the system is far less sensitive to elastic convection suggesting that, in this context, the overall characteristics such as mesh stiffness (average and time variations) can be realistically estimated without considering this phenomenon.

In (1), $k_M(\tau)$ represents the stiffness of an ideal unmodified tooth pair of infinitesimal width dM between engagement and the end of recess i.e., within the interval $\tau \in [0, \varepsilon_\alpha]$ which, following [18], can be expressed as:

$$k_M(\tau) = k_0\left(1 + \alpha\varphi_M(\tau)\right) \qquad (2)$$

where k_0 is the average mesh stiffness per unit contact length (as defined in the ISO 6336 standard [19] for instance), α represents the relative variation in stiffness amplitude and $\varphi_M(\tau)$ accounts for the shape of variation in the meshing course.

By integrating over the time-varying contact length $L(\tau)$, one obtains:

$$k(\tau) = k_0\left[\int_{L(\tau)} dM + \alpha\int_{L(\tau)} \varphi_M(\tau)\, dM\right] \qquad (3)$$

The two integrals in (3) can be replaced by discrete summations over the instantaneous contact lines [18], [20]. Any generic function $f_{00}(\tau)$ representative of a local property (shape deviations, individual stiffness function, etc.) at point M_{00} (entering the edge of the base plane at $\tau = 0$ as shown in Figure 1) is necessarily periodic (i.e. similar meshing conditions will re-occur after a certain period P, integer) and can therefore be developed as a Fourier series of the form:

$$f_{00}(\tau) = \frac{a_0}{2} + \sum_n a_n \cos\left(\frac{2\pi n\tau}{P}\right) + b_n \sin\left(\frac{2\pi n\tau}{P}\right) \qquad (4)$$

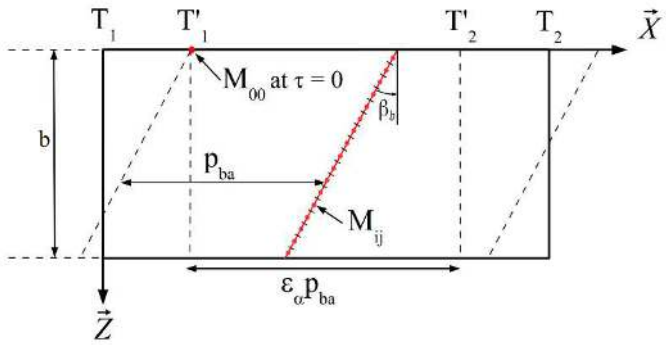

Figure 1 – Point of reference M_{00} on the base plane.

Similar functions can be attached to any other potential contact point M_{ij} (where i refers to the contact line number and j to the segment number on one given contact line) and are derived as:

$$f_{ij}(\tau) = f_{00}\left(\tau - i - \frac{j\varepsilon_\beta}{N}\right) \qquad (5)$$

where N is the number of segments on one complete line of contact of length $b/\cos\beta_b$, b is the face width.

In these conditions, it can be shown that [20]:

$$\lim_{N\to\infty}\left(\frac{1}{N\varepsilon_\alpha}\sum_{i=0}^{P-1}\sum_{j=0}^{N-1}f_{ij}(\tau)\right)=\frac{Pa_0}{2\varepsilon_\alpha}+\sum_{k=1}^{\infty}\frac{\sin(\pi k\varepsilon_\beta)}{\pi k\varepsilon_\beta\varepsilon_\alpha}\left[Pa_{kP}\cos\pi k(2\tau-\varepsilon_\beta)+Pb_{kP}\sin\pi k(2\tau-\varepsilon_\beta)\right] \quad (6)$$

Returning to (3), the first integral can therefore be approximated by:

$$k_0\int_{L(\tau)}dM=\lim_{N\to\infty}\left(k_0\sum_{i=0}^{P-1}\sum_{j=0}^{N-1}\frac{b}{\cos\beta_b}\frac{1}{N}\pi_{ij}(\tau)\right)=k_{m0}\lim_{N\to\infty}\left(\frac{1}{N\varepsilon_\alpha}\sum_{i=0}^{P-1}\sum_{j=0}^{N-1}\pi_{ij}(\tau)\right) \quad (7)$$

where $k_{m0}=k_0\frac{b\varepsilon_\alpha}{\cos\beta_b}$ represents the average mesh stiffness with constant stiffness per unit contact length k_0 and $\pi_{ij}(\tau)$ is a windowing function which is 1 when M_{ij} lies in the active contact zone in the base plane and 0 otherwise.

Similar developments are possible with $\alpha k_0\int_{L(\tau)}\varphi_M(\tau)dM$ providing that the time variations of $\varphi_M(\tau)$ are specified. Based on the results of [1], a parabolic variation appears as sufficiently representative and is used here so that:

$$\varphi_{M_{00}}(\tau)\cong A+B\tau+C\tau^2 \quad (8)$$

Combining (3), (6), (7), (8), the following dimensionless time-varying mesh stiffness function can be obtained:

$$\hat{k}(\tau)=1+\sum_{k=1}^{\infty}\frac{Sinc(k\varepsilon_\beta)}{\pi k\varepsilon_\alpha}\cdot\left[\begin{array}{l}2\sin(\pi k\varepsilon_\alpha)\cos\left(\pi k(2\tau-\varepsilon_\alpha-\varepsilon_\beta)\right)\\+\alpha\left(-A+\frac{C}{2\pi^2k^2}\right)\sin\left(\pi k\left(-2\tau+\varepsilon_\beta\right)\right)\\+\alpha\left(A+B\varepsilon_\alpha+C{\varepsilon_\alpha}^2\left(1-\frac{1}{2\pi^2k^2{\varepsilon_\alpha}^2}\right)-\right)\\*\sin\left(\pi k\left(2\varepsilon_\alpha-2\tau+\varepsilon_\beta\right)\right)\\+\alpha\left(-\frac{B}{2\pi k}\right)\cos\left(\pi k\left(-2\tau+\varepsilon_\beta\right)\right)\\+\alpha\left(\frac{B}{2\pi k}+\frac{C\varepsilon_\alpha}{\pi k}\right)\cos\left(\pi k\left(2\varepsilon_\alpha-2\tau+\varepsilon_\beta\right)\right)\end{array}\right] \quad (9)$$

where $\hat{k}(\tau)=\frac{k(\tau)}{k_{m0}}$ and $Sinc(x)=\frac{\sin(\pi x)}{\pi x}$ is the classic sine cardinal function.

It can be verified that, when $\alpha=0$, (9) reduces to the analytical expression of the dimensionless contact length proposed by Maatar and Velex [21]. Without any loss of generality, it can be remarked that:

a) the time-varying parts of $\hat{k}(\tau)$ are proportional to $Sinc(k\varepsilon_\beta)$ which is zero for integral values of ε_β (since k is necessarily an integer).
b) as opposed to a model with constant stiffness per unit contact length, integral profile contact ratios ε_α do not eliminate mesh stiffness variations when $\alpha\neq0$ although the contact length is theoretically constant.

A more practical and concise design formula can be derived if realistic values of the unknown coefficients α, A, B and C can be estimated. Concerning the coefficient *A*, *B* and *C* of the parabolic function $\varphi_{M_{00}}(\tau)$, it is further assumed that the tooth pair stiffness for any thin (infinitesimal) spur gear is reasonably symmetric between engagement and the end of recess. Normalizing the shape function such that $\varphi_{M_{00}}(\tau=0)=\varphi_{M_{00}}(\tau=\varepsilon_\alpha)=-1$ and using the fact that $\int_0^{\varepsilon_\alpha}\varphi_M(\tau)d\tau=0$, one obtains $A=-1,\ B=6/\varepsilon_\alpha,\ C=-6/\varepsilon_\alpha^2$. With regard to the relative amplitude factor α, its value has been calculated for a number of gear geometries, using *i*) the classic equations of Weber and Banaschek (based on numerical integrations in order to take into account the exact tooth geometry) [1], *ii*) the analytical formula of Cai and Hayashi for one tooth pair stiffness [22] and, *iii*) the inverse unit potential introduced by Pedrero et al. [23]. It has been found that all the results lie in the range $\alpha\in$ [0.25 – 0.35] and an average value of $\alpha=0.3$ has been retained.

In these conditions, the approximate mesh stiffness equation in (9) can be largely simplified and reduces to:

$$\hat{k}(\tau)=1+2\sum_{k=1}^{\infty}\Xi_k(\varepsilon_\alpha)Sinc(k\varepsilon_\beta)\cos\left(\pi k(2\tau-\varepsilon_\alpha-\varepsilon_\beta)\right) \quad (10)$$

with $\Xi_k(\varepsilon_\alpha)\cong\left(0.7+\frac{0.09}{k^2\varepsilon_\alpha^2}\right)Sinc(k\varepsilon_\alpha)-\frac{0.09}{k^2\varepsilon_\alpha^2}\cos(\pi k\varepsilon_\alpha)$

II COMPARISONS WITH NUMERICAL SIMULATIONS

The validity of formulae (9) and (10) has been assessed by comparison with finite elements results derived from refined 2D models and benchmark results from the literature.

II.1 2D Finite Elements results

Two finite element (FE) models have been set up (Figure 2) which represent either i) a complete pinion whose displacements at the nodes around the bore are blocked (inner

radius) or ii) a sector of a pinion or a gear comprising 5 successive teeth with the nodes blocked on the inner radius and lateral sides.

The two models have the same node density and, for both, a highly refined FE grid is introduced on the loaded tooth thus making it possible to introduce the Hertzian pressure distribution directly at various locations along the tooth profile as opposed to the lumped forces currently employed. By so doing, singular displacement fields are avoided and so is the questionable (though often used) decomposition into contact and structural deflections (as is the case in WB formulae and the FE results in [14-16] for instance). The external loading is determined based on the classic Hertzian analytical results for cylinder-on-cylinder contacts and the influence of tooth bending on the contact extent and pressure distribution is therefore neglected. The displacement normal to the profile at the center of the semi-elliptical pressure distribution is used to determine the pinion tooth stiffness function which is then combined in series with that of the other mating member. Finally, the tooth pair stiffness functions are phased and superimposed to account for single and double tooth contacts and give the overall mesh stiffness. For the results in Figure 3, the inner radius where all the displacements are blocked is conventionally taken as the root radius minus four modules on both the pinion and the gear. The comparison examples in Figure 3 for cases 1 and 2 as defined in Table 1 show that the analytical formula (10) is actually representative of the mesh stiffness variations even when there is no exact symmetry between the condition at engagement and the end of recess as is the case for the 25/83 example. It can also be noticed that the mesh stiffness variations with respect to the average mesh stiffness is almost insensitive to the model used (full pinion or sector).

Table 1 – Gear data

case	α_0(°)	β(°)	$Z_1;Z_2$	$b_1;b_2$ (mm)	ε_α	ε_β	ρ^*
1	20	0	25; 25	10; 10	1.721	0	0.4
2	20	0	25; 83	10; 10	1.612	0	0.4
3	20	0	25; 33	95; 90	1.59	0	0.4
4	20	8	26; 141	158; 150	1.67	1.33	0.35

II.2 Quasi-analytical formulae (WB) and LDP results

The dimensionless mesh stiffness $\hat{k}(\tau)$ (mesh stiffness divided by the average mesh stiffness over one mesh period) for another spur gear example (case 3 in Table 1) has also been derived:

i) from the numerical integration of the formulae of Weber & Banaschek [1],

ii) using the Load Distribution Program (LDP) developed at Ohio State University [24-26] and considered as a benchmark code for quasi-static gear simulations

iii) based on formulae (9) and (10)

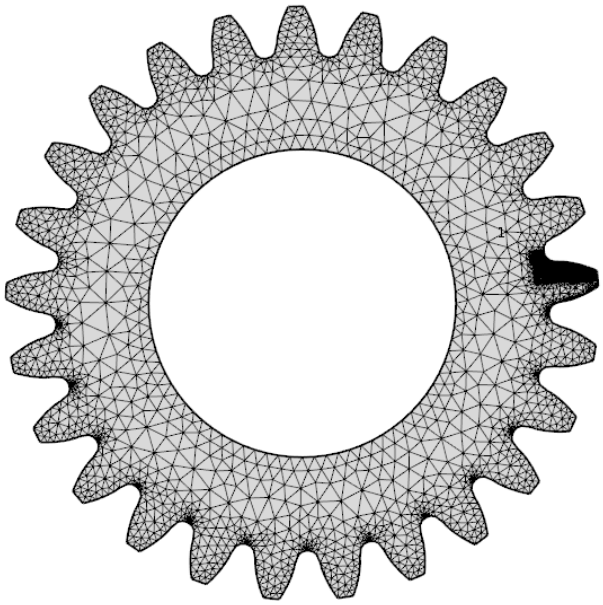

a – FE model for a complete pinion

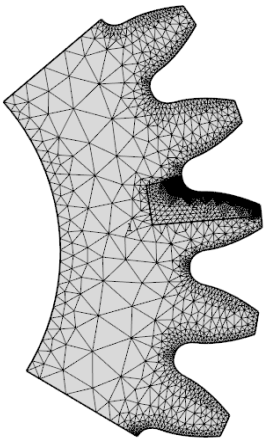

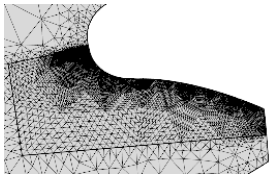

b- FE mesh for a 5-tooth sector

c- Loaded profile (detail)

Figure 2 – Finite element models.

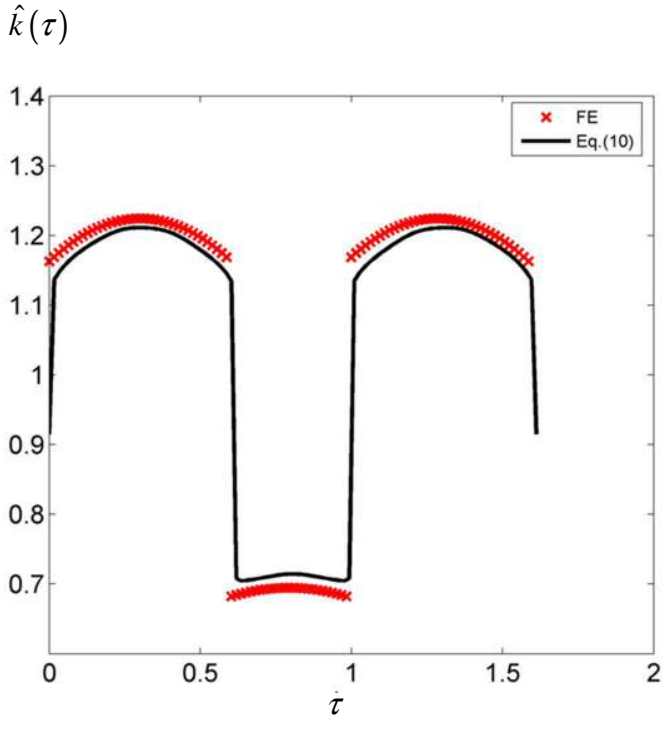

a- 25/25 pinion – gear (full FE model)

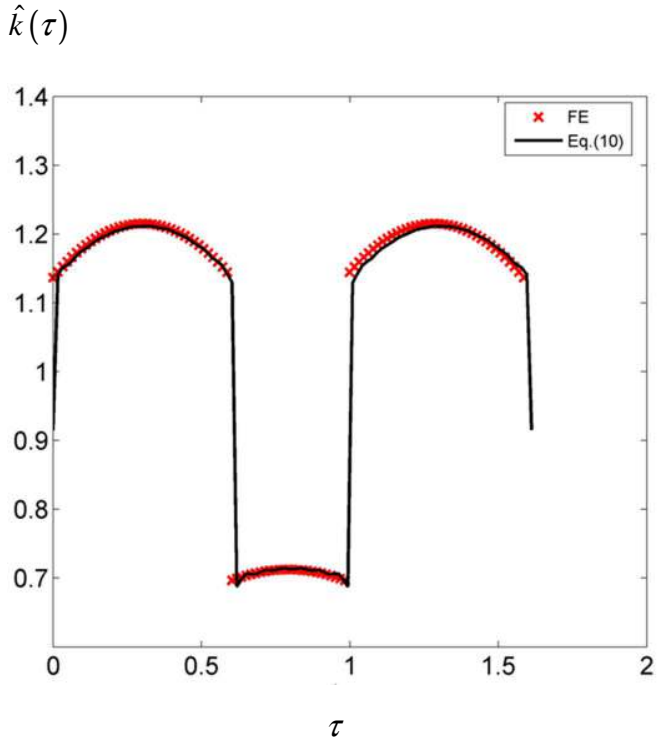

b- 25/25 pinion-gear (5-tooth sector)

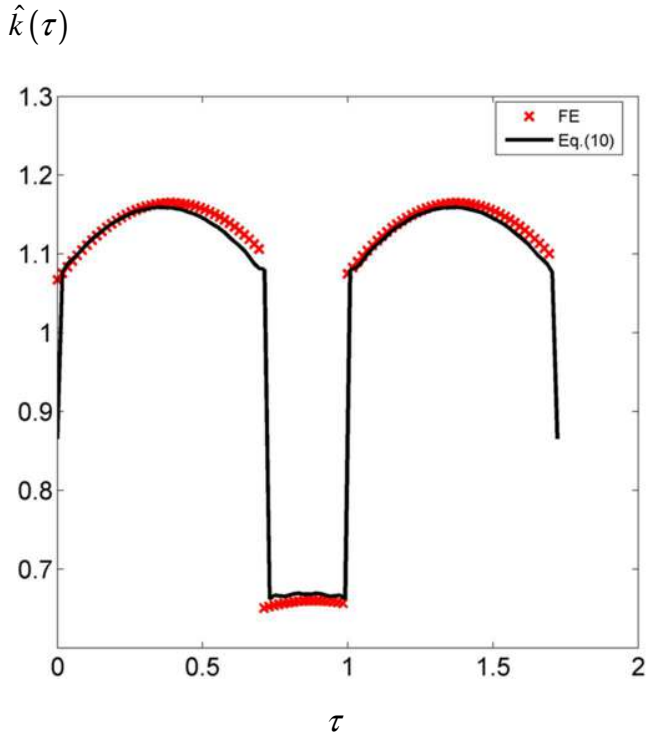

c- 25/83 pinion-gear (5-tooth sector)

Figure 3 – Dimensionless mesh stiffness functions – Comparisons between FE results and (10).

The series of results in Figure 4 are all in very good agreement showing, indirectly, that the time variations of the mesh stiffness as derived from the analytical expressions of WB agree well with finite element results for 2D models. Comparisons have been extended to helical gears (case 4 in Table 1) by calculating the dimensionless mesh stiffness functions in Figure 5. Here again, the four curves are similar thus indicating that the proposed analytical expressions are sound. Finally, the sensitivity to the value of α has been analyzed and it has been found that the approximate value $\alpha = 0.3$ is a good compromise and leads to accurate results over a broad range of gear geometries.

III GEAR GEOMETRY AND PARAMETRIC EXCITATIONS

Interestingly, formula (10) reveals that mesh stiffness time variations for ideal gears mostly depend on 2 parameters only: the profile and face contact ratio ε_α and ε_β, so that general diagrams of parametric excitation amplitudes for all spur and helical gears (within the limits of the proposed theory) can be drawn. The corresponding level curves of the RMS of $\hat{k}(\tau)$

are plotted in Figure 6 whereas Figure 7 shows the results associated with the first four harmonics of the mesh frequency.

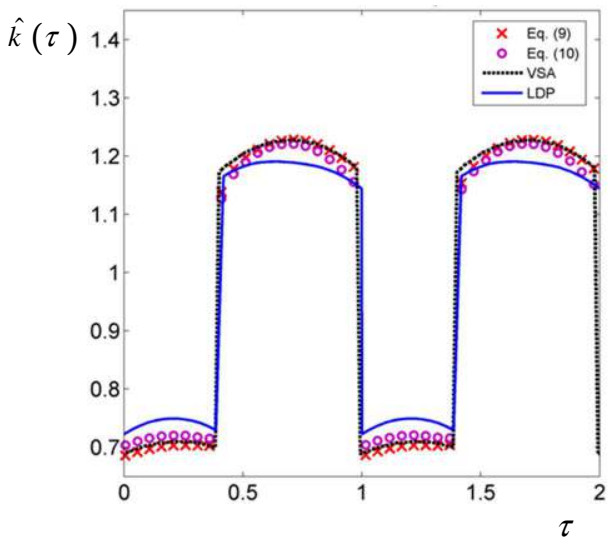

Figure 4 – Comparisons between (9), (10), the numerical integration of Weber & Banaschek's formulae (referred to as VSA) and the results from LDP.
Spur gear example (25/33)

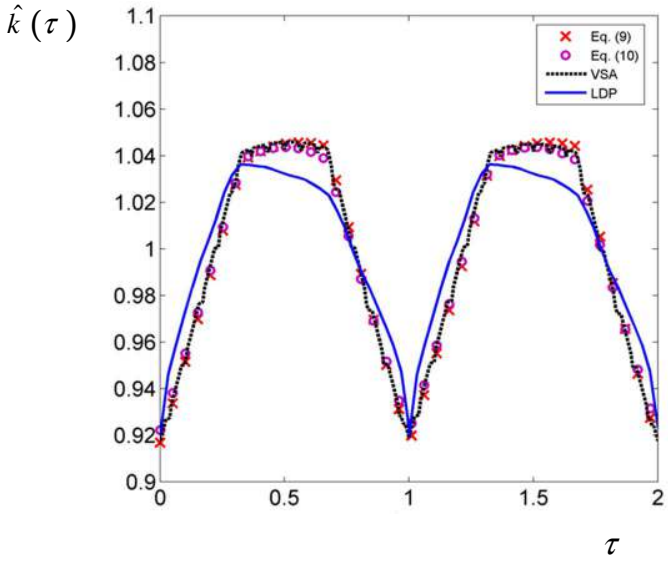

Figure 5 – Comparisons between (9), (10), the numerical integration of Weber & Banaschek's formulae (referred to as VSA) and the results from LDP.
Helical gear example (26/141)

The general trends are rather similar to those found using the level curves of the RMS of contact length [21] with some noticeable differences on the influence of profile contact ratios since $\varepsilon_\alpha = 2$ does not entirely eliminate parametric excitations although integral face and profile contact ratios certainly remain favorable. Most of the excitation amplitude is associated with the first harmonic of the mesh frequency but higher harmonics can contribute too, especially for some particular profile contact ratios with the cancellation of some excitation harmonics.

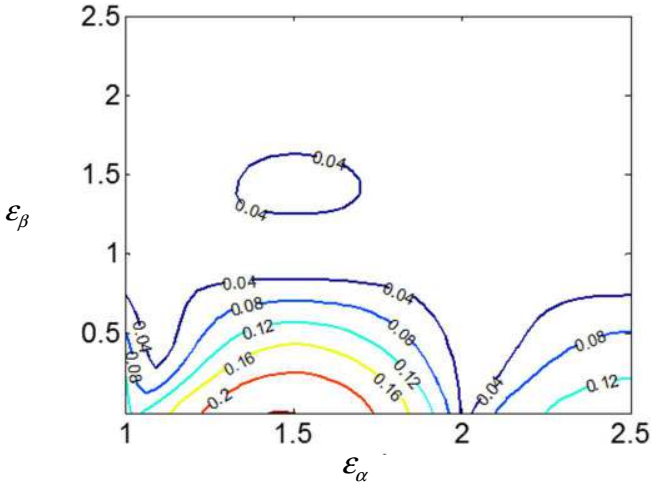

Figure 6- Contour plots of the RMS of $\hat{k}(\tau)$ (using (10)) for various profile (ε_α) and transverse (ε_β) contact ratios.

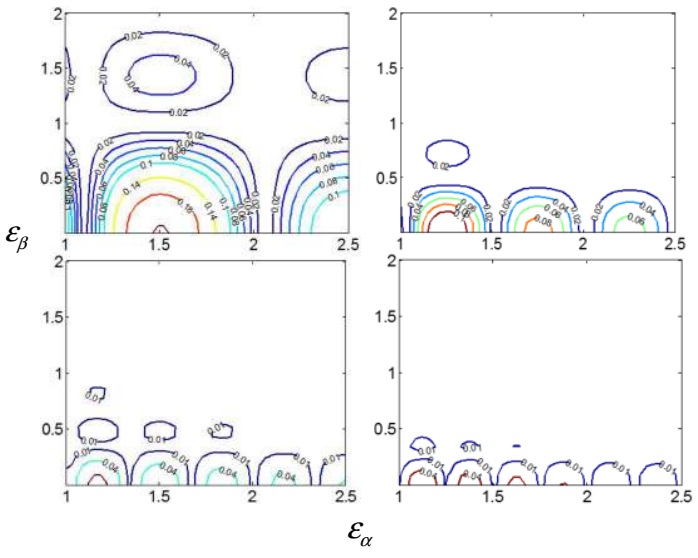

Figure 7 - Contour plots of the RMS of $\hat{k}(\tau)$ using (10) for the first 4 mesh harmonics versus profile and transverse contact ratios.

IV DISCUSSION – CLOSURE

Some analytical formulae have been proposed which seem to capture most of the mesh stiffness time variations (parametric excitations) for ideal solid spur and helical gears. The simplified equation (10) indicates that mesh stiffness fluctuations are mostly controlled by the profile and face contact ratios which makes it possible to draw performance diagrams for any spur and helical gear geometry. These results are clearly approximate but it is believed that they can give reasonable estimates of the mesh stiffness functions useful for gear dynamic simulations in particular. However, if the proposed dimensionless mesh stiffness formulae agree well with FE and benchmark results from the literature, there is greater discrepancy when it comes to the actual stiffness function (i.e., when multiplying by the average mesh stiffness).

Depending on the gear example and model, somewhat different values of mesh stiffness per unit contact length k_0 need to be employed in order to match the results derived from (9) and (10) with those from FE, WB, LDP as illustrated in Table 2 (for completeness, the value of k_0 given by the ISO 6336 formula [4] has been added). Part of the scatter can be explained by the influence of gear body elasticity since k_0 derived from the finite element results appears as sensitive to the boundary conditions depending on the bore radius and if the full pinion or only a 5-tooth sector is considered. It can be noticed that significant variations of k_0 are observed although the relative stiffness variations (in Figure 3) are unchanged. Further elements can be found in [5] concerning the different modelling strategies of the so-called foundation effects and their influence on mesh stiffness.

Table 2 – Mesh stiffness per unit contact length k_0 for various gear geometries and models.

case	$(k_0/E10)$ N/m^2 (ISO 6336)	$(k_0/E10)$ N/m^2 (WB)	$(k_0/E10)$ N/m^2 (FE)	$(k_0/E10)$ N/m^2 (LDP)
1	1.255	1.436	$1.372^{(a)}$ / $1.473^{(b)}$ / $1.587^{(c)}$	-
2	1.414	1.539	$1.652^{(a)}$ / $1.806^{(b)}$	-
3	1.343	1.479	-	1.237
4	1.481	1.414	-	1.235

$^{(a)}$ *: full pinion model with bore radius equals root radius – 4 modules;*

$^{(b)}$ *: 5-tooth sector model with bore radius equals root radius – 4 modules;*

$^{(c)}$ *: 5-tooth sector model with bore radius equals root radius –2 modules.*

Another drawback of the proposed methodology concerns the influence of profile/lead modifications which can substantially modify the mesh stiffness function for loads below the design load thus leading to reduced actual profile and face contact ratios. Some analytical expressions are possible but their complexity renders numerical solutions preferable and, in a way, easier to implement.

REFERENCES

[1] Weber, C., and Banaschek, K., 1953, *Formänderung und Profilrücknahme bei Gerad-und Schrägverzahnten Antriebstechnik*, Vieweg, Braunschweig, Vol. 11.

[2] Attia, A.Y., 1964, "Deflection of Spur Gear Teeth Cut in Thin Rims", J. Manuf. Sci. Eng. 86(4), pp. 333-341, doi:10.1115/1.3670554

[3] Cornell, R. W., 1981, "Compliance and Stress Sensitivity of Spur Gear Teeth", J. Mech. Des., 103(2), pp. 447-459, doi:10.1115/1.3254939

[4] Winter, H. and Podlesnik, B., 1983, "Zahnfedersteifigkeit von Stirnrad-paaren, Teil 1 to 3". Antriebstechnik, **22** (3), pp. 39–42 (Teil 1), **22** (5), pp. 51–58 (Teil 2), **23** (11), pp. 43–49 (Teil 3).

[5] Sainsot, P., Velex, P. and Duverger, O., 2004, "Contribution of Gear Body to Tooth Deflections—A New Bidimensional Analytical Formula", J. Mech. Des., 126 (4), pp. 748-752. doi:10.1115/1.1758252

[6] Wilcox, L. and Coleman, W., 1973, "Application of Finite Elements to the Analysis of Gear Tooth Stresses", J. Manuf. Sci. Eng. 95(4), pp. 1139-1148. doi:10.1115/1.3438262

[7] Chabert, G., Dang Tran, T. and Mathis, R., 1974, "An evaluation of Stresses and Deflections of Spur Gear Teeth under Strain", J. Manuf. Sci. Eng. **96**(1), pp. 85-93. doi:10.1115/1.3438335

[8] Umezawa, K., 1972, "Deflections and moments due to a concentrated load on a rack-shaped cantilever plate with finite width for gears", Bulletin of JSME, **15**(79), pp. 116-130.

[9] Yau, E., Busby H.R. and Houser D.R., 1994, "A Rayleigh-Ritz approach to modeling bending and shear deflections of gear teeth", Computers & Structures, **50** (5), pp. 705-713. doi: 10.1016/0045-7949(94)90429-4

[10] Cai, Y., 1995," Simulation of the rotational vibration of helical gears in consideration of the tooth separation phenomenon (A new stiffness function of helical involute tooth pair)", J. Mech. Des., **117**(3), pp. 460-469. doi:10.1115/1.2826701

[11] Seager, D. L., 1967, "Some elastic effects in helical gears', PhD Cambridge University, 209 p.

[12] Schmidt G. R., Pinnekamp W. and Wunder A., 1980, "Optimal tooth profile correction of helical gears", *Proc. of the*

Third International Power Transmissions and Gearing Conference, San Francisco, California, paper DET-110.

[13] Ajmi, M. and Velex, P., 2005, "A model for simulating the quasi-static and dynamic behaviour of solid wide-faced spur and helical gears", Mechanism and Machine Theory, **40** (2), pp. 173-190. doi: 10.1016/j.mechmachtheory.2003.06.001

[14] Vedmar, L., 1981, "On the design of external involute helical gears", PhD Lund Technical University, 100 p.

[15] Steward, J. H., 1989, "Elastic analysis of load distribution in wide-faced spur gears", PhD University of Newcastle, 208 p.

[16] Haddad, C. D., 1991, "The elastic analysis of load distribution in wide-faced helical gears", PhD University of Newcastle, 470 p.

[17] Smith, J. D., 2003, *Gear Noise and Vibration*, Marcel Dekker, Cambridge, pp. 35-40. ISBN: 0-8247-4129-3

[18] J. Bruyère, P. Velex, Derivation of optimum profile modifications in narrow-faced spur and helical gears using a perturbation method, Journal of Mechanical Design **135** (7) (2013), 8 pages, doi: 10.1115/1.4024374.

[19] ISO/DIS 6336-2 &3, 2004, "*Calculation of Load Capacity of Spur and Helical Gears—Parts 2 & 3*", International Organization for Standardization, Geneva, Switzerland.

[20] Velex, P. Sainsot P., 2002, "An analytical study of tooth friction excitations in errorless spur and helical gears", Mechanism and Machine Theory, **37**(7), pp. 641-658.

[21] Maatar M. and Velex P., 1996, "An analytical expression of the time-varying contact length in perfect cylindrical gears - Some possible applications in gear dynamics", J. Mech. Des., **118** (4), pp. 586-589.

[22] Cai, Y. and Hayashi, T., 1992, "The optimum modification of tooth profile for a pair of spur gears to make its rotational vibration equal zero", *Proc. 6th ASME Int. Power Trans. and Gearing Conference*, Phoenix, pp. 453-460.

[23] Pedrero J. I., Vallejo I. I. and Pleguezuelos M., 2007, "Calculation of tooth bending strength and surface durability of high transverse contact ratio spur and helical gear drives", J. Mech. Des. **129** (1) pp. 69-74.

[24] Houser D. R., Harianto J., Iyer N., Josephson J. and Chandrasekaren B., 2000, "A multi-variable approach to determining the 'best' gear design", *Proc. 8th ASME International Power Transmission and Gearing Conference*, Baltimore, Sept. 10-13, 8 pages.

[25] Sundaresan S., Ishii K., and Houser D. R., 1991,"A Procedure Using Manufacturing Variance to Design Gears With Minimum Transmission Error", J. Mech. Des. **113** (3) pp. 318-325. doi:10.1115/1.2912785

[26] Sundaresan, S., Ishii, K., Houser, D.R., 1992, "Design Optimization for Robustness Using Performance Simulation Programs", Engineering Optimization, **20**(3) pp. 163-178. doi:10.1080/03052159208941